Hepatocellular Carcinoma: Signal Intensity at Gadoxetic Acid–enhanced MR Imaging—Correlation with Molecular Transporters and Histopathologic Features[1]

Azusa Kitao, MD
Yoh Zen, MD
Osamu Matsui, MD
Toshifumi Gabata, MD
Satoshi Kobayashi, MD
Wataru Koda, MD
Kazuto Kozaka, MD
Norihide Yoneda, MD
Tatsuya Yamashita, MD
Shuichi Kaneko, MD
Yasuni Nakanuma, MD

Purpose: To analyze the correlation between signal intensity in the hepatobiliary phase of gadoxetic acid–enhanced magnetic resonance (MR) imaging and the expression of hepatocyte transporters with histopathologic features in hepatocellular carcinoma (HCC).

Materials and Methods: Institutional ethics committee approval and informed consent were obtained. Forty surgically resected HCCs were classified as hypointense (n = 32) or iso- or hyperintense (n = 8) on the basis of findings in the hepatobiliary phase of gadoxetic acid–enhanced MR imaging. The following were compared between hypointense and iso- or hyperintense HCCs: the time–signal intensity curves at gadoxetic acid–enhanced MR imaging, the expression levels of seven transporters (four organic anion–transporting polypeptides [OATPs] and three multidrug-resistant proteins [MRPs]) at polymerase chain reaction (PCR) (for 22 nodules), results of immunostaining of OATP8, and histologic features. Statistical analysis (unpaired t test, Mann-Whitney test, χ^2 test, and Fisher exact test) was performed for each result.

Results: On the time–signal intensity curves, hypointense HCCs showed a decreasing pattern, whereas iso- or hyperintense HCCs showed an increasing pattern after the dynamic phase. PCR revealed that expression of OATP8 (an uptake transporter) in hypointense HCCs was lower and that in iso- or hyperintense HCCs was higher than in background liver ($P < .001$). The expression level of MRP3 (a sinusoidal export transporter) showed a similar trend to that of OATP8 ($P < .001$). Immunostaining revealed that OATP8 expression was weak in hypointense HCCs, whereas it was sustained in iso- or hyperintense HCCs ($P < .001$). At histologic examination, a pseudoglandular proliferation pattern with bile plugs was more commonly observed in iso- or hyperintense HCCs than in hypointense HCCs (P = .01 for proliferation patterns and P = .006 for bile plugs).

Conclusion: The enhancement ratio of HCCs in the hepatobiliary phase of gadoxetic acid–enhanced MR imaging positively correlated with expression levels of OATP8 and MRP3, indicating that gadoxetic acid is taken up by OATP8 and excreted by MRP3.

Supplemental material: *http://radiology.rsna.org/lookup/suppl/doi:10.1148/radiol.10092214/-/DC1*

[1] From the Departments of Radiology (A.K., O.M., T.G., S. Kobayashi, W.K., K.K., N.Y.), Human Pathology (A.K., Y.Z., Y.N.), and Gastroenterology (T.Y., S. Kaneko), Kanazawa University Graduate School of Medical Science, 13-1 Takara-machi, Kanazawa 920-8640, Japan. Received November 24, 2009; revision requested January 6, 2010; revision received February 25; accepted March 24; final version accepted April 28. Supported in part by a Grant-in-Aid for Scientific Research (no. 21591549) from the Ministry of Education, Culture, Sports, Science and Technology, Tokyo, Japan and by Japanese Health and Labor Sciences research grants for the development of novel molecular markers and imaging modalities for earlier diagnosis of hepatocellular carcinoma. **Address correspondence to** A.K. (e-mail: *kitao@rad.m.kanazawa-u.ac.jp*).

Gadoxetic acid is a recently developed hepatobiliary-specific contrast material for magnetic resonance (MR) imaging that has high sensitivity in the detection of malignant liver tumors (1–7). Because gadoxetic acid is taken up by hepatocytes and then excreted into the bile ducts (8), hepatic focal lesions without normal hepatobiliary function can be definitively depicted as hypointense areas compared with the well-enhanced hyperintense background liver in the hepatobiliary phase of gadoxetic acid–enhanced MR imaging (1,9). In addition, gadoxetic acid can be used in the same way as gadopentetate dimeglumine to evaluate the hemodynamics of hepatic lesions in the dynamic phase after an intravenous bolus injection (1,2,4–6).

Classically, hepatocellular carcinomas (HCCs) commonly show rapid enhancement in the arterial dominant phase and a decrease in signal intensity (SI) from the portal dominant phase to the equilibrium phase. This decreasing pattern corresponds to the decline of contrast material in the tumor blood spaces, or so-called washout (10). In the hepatobiliary phase of gadoxetic acid–enhanced MR imaging, most HCCs are hypointense, although hyperintense HCCs are also sometimes encountered (4,7). Elucidating the mechanisms of this difference in imaging appearance may be important in the detection and characterization of HCCs. However, the uptake and excretion of gadoxetic acid in human liver and hepatic tumors have not been well analyzed (11,12).

In a rat experimental study, the hepatic uptake transporter of gadoxetic acid was confirmed to be organic anion–transporting polypeptide (OATP) 1 (13), and the export transporter was multidrug-resistant protein (MRP) 2 (14). However, the results obtained in rats cannot necessarily be easily applied to humans. Substrates transported by rat OATP1 can be taken up by OATP-A, OATP-B, OATP-C, and OATP8, which are also expressed on the sinusoidal side of human hepatocytes (15–20). Regarding export transporters, MRP2 in rat liver is considered to be an homologue to MRP2 in human liver, which is expressed on the canalicular side of hepatocytes (21–23). In addition, MRP1 and MRP3 on the sinusoidal side of human hepatocytes can also export some of the substrates of MRP2 (22,24). These seven transporters carry organic anions containing many kinds of intrinsic or extrinsic molecules—for example, a component of bile acid, hormones, and several drugs (15–24). Gadoxetic acid is also an organic anion, and therefore we expected that some of those transporters would be involved in the uptake and excretion of this contrast material in human liver and HCCs.

We performed this study to analyze the correlation between SI in the hepatobiliary phase of gadoxetic acid–enhanced MR imaging and the expression of hepatocyte transporters with histopathologic features in HCC.

Advances in Knowledge

- The expressions of the hepatocyte membrane uptake transporter organic anion–transporting polypeptide 8 (OATP8) and the export transporter multidrug-resistant protein 3 (MRP3) significantly correlate with the signal intensity of hepatocellular carcinomas (HCCs) in the hepatobiliary phase of gadoxetic acid–enhanced MR imaging ($P < .001$).
- On human HCC cells, OATP8 and MRP3 are the most probable uptake transporter and export transporter of gadoxetic acid, respectively.
- At histologic examination, a pseudoglandular proliferation pattern with bile plugs was observed with significantly high frequency in HCCs that were iso- or hyperintense in the hepatobiliary phase of gadoxetic acid–enhanced MR imaging ($P < .01$).
- The time–signal intensity curve of HCCs at gadoxetic acid–enhanced MR imaging can differ between hypointense HCCs and iso- or hyperintense HCCs ($P < .001$).

Implication for Patient Care

- When we encounter iso- or hyperintense HCCs in the hepatobiliary phase of gadoxetic acid–enhanced MR imaging, we can speculate that the pathologic examination will show a pseudoglandular proliferation pattern and bile plugs.

Materials and Methods

Patients

This retrospective study was performed with the approval of the institutional ethics committee, and informed consent for use of the MR images and the resected specimens was obtained from all patients. Forty-nine HCCs in 47 patients were surgically resected at our institution from April 2008 to June 2009. We excluded nine HCCs in nine patients, including three patients who did not undergo gadoxetic acid–enhanced MR imaging because of renal failure and three patients with a history of previous treatment for HCC, including ablation therapy or transarterial chemoembolization therapy. One pathologist (Y.Z., with 11 years of experience) and one abdominal imaging radiologist (A.K., with 8 years of experience) evaluated and excluded three HCCs with necrosis, hemorrhage, and/or cystic degeneration

Published online before print
10.1148/radiol.10092214

Radiology 2010; 256:817–826

Abbreviations:
HCC = hepatocellular carcinoma
MRP = multidrug-resistant protein
OATP = organic anion–transporting polypeptide
PCR = polymerase chain reaction
ROI = region of interest
SI = signal intensity

Author contributions:
Guarantors of integrity of entire study, A.K., O.M., T.G., S. Kaneko, Y.N.; study concepts/study design or data acquisition or data analysis/interpretation, all authors; manuscript drafting or manuscript revision for important intellectual content, all authors; manuscript final version approval, all authors; literature research, A.K.; clinical studies, A.K., O.M., T.G., S. Kobayashi, W.K., K.K., T.Y.; experimental studies, A.K., Y.Z., N.Y., T.Y., S. Kaneko, Y.N.; statistical analysis, A.K.; and manuscript editing, A.K., Y.Z., O.M., Y.N.

Authors stated no financial relationship to disclose.

See also the article by Tsuda and Matsui in this issue.

covering more than one-fourth of the entire lesion at histologic examination. Therefore, our final study comprised 40 HCCs in 38 patients. Mean patient age was 63.0 years ± 10.4 (standard deviation) (range, 38–81 years) for the entire study group, 63.0 years ± 11.0 (range, 38–81 years) for men, and 63.0 years ± 9.4 (range, 43–78 years) for women. The male:female ratio was 26:12 (68%:32%), and 34 (89%) of 38 patients had chronic liver disease (Table 1). Hepatic function was preserved in all patients, and all patients with liver cirrhosis had grade A cirrhosis according to the Child classification.

Table 1

Clinical Features of Patients

Feature	Hypointense HCC	Iso- or Hyperintense HCC
No. of tumors	32	8
Resected tumor size (cm)	4.2 ± 2.9 (0.7–14.5)	4.0 ± 2.9 (2.2–10.5)
Age (y)	61.8 ± 10.3 (38–78)	66.0 ± 10.8 (51–81)
Male-to-female ratio*	22:10	6:2
Background liver tissue*		
Chronic hepatitis	9 (One patient with HBV, six with HCV, and two with cryptogenic hepatitis)	2 (Both patients had HCV)
Liver cirrhosis	18 (Four patients with HBV, nine with HCV, two with NASH, one with AIH, and two with cryptogenic cirrhosis)	5 (One patient with HBV, one with HCV, two with NASH, and one with cryptogenic cirrhosis)
Normal liver	5	1

Note.—Unless otherwise specified, data are means ± standard deviations, with ranges in parentheses. No significant differences were observed in any clinical features between the two types of HCCs (size: $P = .84$; age: $P = .32$; sex: $P > .99$; background liver: $P = .95$. AIH = autoimmune hepatitis, HBV = hepatitis B virus, HCV = hepatitis C virus, NASH = nonalcoholic steatohepatitis.

* Data are numbers of patients.

Gadoxetic Acid–enhanced MR Imaging

Gadoxetic acid–enhanced MR imaging was performed before surgical resection (mean time before surgery, 52.8 days ± 25.3 [range, 3–95 days]) for the characterization and pretreatment staging of HCC. MR images were obtained with either a 1.5-T (n = 15) or 3.0-T (n = 25) MR system (Signa HDx; GE Medical Systems, Milwaukee, Wis) by using the same protocol. MR imaging was performed with a fat-suppressed three-dimensional T1-weighted spoiled gradient echo in the steady state sequence (liver acquisition with volume acceleration extended version, generalized encoding matrix; repetition time msec/echo time msec, 3.4–3.6/1.6; flip angle, 12°–15°; field of view, 42 × 42 cm; matrix, 192 × 320 interpolated to 512 × 512; section thickness, 4.2 mm; and overlap, 2.1 mm). For the dynamic study, a dose of 0.1 mL of Primovist (0.25 mmol/mL of gadoxetic acid, Bayer Schering Pharma, Berlin, Germany) per kilogram of body weight was intravenously injected at a flow rate of 1.0 mL/sec (25), followed by a 30-mL saline flush. We used the test injection method (1.5 mL of gadoxetic acid plus an 8-mL saline flush) to determine the optimal arterial dominant phase, which was determined as the peak time of enhancement in the abdominal aorta plus an additional 10 seconds of imaging time (16–22 seconds) · ½. After imaging in the arterial phase, portal phase and equilibrium phase images were obtained 20 and 60 seconds after the previous imaging phase was finished, respectively. The hepatobiliary phase was imaged 20 minutes after the injection in all patients. In 27 patients, imaging was performed in an additional phase 15 minutes after the injection.

Analysis of SI on Gadoxetic Acid–enhanced MR Images

Image analysis was performed in consensus by two abdominal imaging radiologists (A.K. and O.M. [with 38 years of experience]). The SIs of the tumor and surrounding background liver were measured by placing regions of interest (ROIs). The ROI of the tumor was determined as the maximum oval or round area at the level of the largest diameter of the tumor, and the average ROI size was 923.6 mm^2 ± 1418.3 (range, 61–6167 mm^2). For both nodules with homogeneous SI and nodules with heterogeneous SI, the average intensity of the entire area was used for analysis. A similarly sized ROI was set over the adjacent liver parenchyma, avoiding the large vessels. ROIs were measured in the arterial, venous, equilibrium, and delayed phases.

Classification of HCCs in the Hepatobiliary Phase of Gadoxetic Acid–enhanced MR Imaging

The HCC nodules were retrospectively classified into two types according to the SI measurement in the hepatobiliary phase of gadoxetic acid–enhanced MR imaging—namely, hypointense HCCs and iso- or hyperintense HCCs. Hypointense HCCs had lower SIs (tumor SI/background SI < 0.9) in the hepatobiliary phase (Fig 1a; Fig E1 [online]). Iso- or hyperintense HCCs had the same or higher SIs (tumor SI/background SI ≥ 1.0) (Fig 1b). There was no intermediate case (tumor SI/background SI = 0.9–1.0). In this study, all HCCs demonstrated hypointensity relative to the surrounding liver on precontrast T1-weighted images, and therefore all iso- or hyperintense HCCs were considered to be enhanced in the hepatobiliary phase of gadoxetic acid–enhanced MR imaging.

Time-SI Curve at Gadoxetic Acid–enhanced MR Imaging

To assess the degree and time course of gadoxetic acid uptake and/or export, we measured the SI at the maximum cross section of each ROI in the precontrast, arterial, portal, equilibrium, and hepatobiliary phases. We calculated the enhancement ratio [(postenhancement SI minus pre-enhancement SI)/pre-enhancement SI] at each time point and traced time-SI curves with software (Prism5; GraphPad Software, San Diego, Calif). One radiologist (A.K.) performed this analysis.

Histologic Diagnosis

Hematoxylin-eosin staining of tissue slices was performed for all 40 liver specimens.

Figure 1

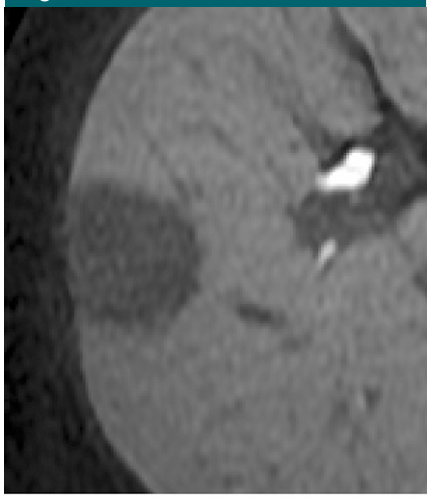

a.

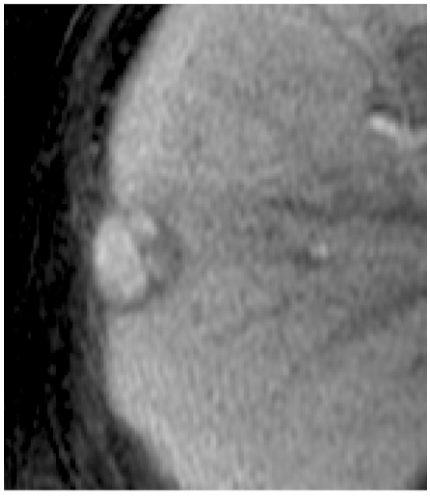

b.

Figure 1: Typical findings of the two types of HCC in the hepatobiliary phase of gadoxetic acid–enhanced axial MR imaging. **(a)** On image obtained in the hepatobiliary phase (20 minutes after injection of gadoxetic acid) in a 62-year-old woman, a hypointense HCC shows definitely lower SI. **(b)** In contrast, image of iso- or hyperintense HCC obtained in 66-year-old man shows almost higher SI, with a portion showing lower SI relative to the surrounding enhanced liver.

Two pathologists (Y.Z. and Y.N. [with 37 years of experience]) diagnosed each nodule according to the classification proposed by the International Working Party (26) and the World Health Organization classification (27): well, moderately, or poorly differentiated HCC. Then, HCCs were classified into four proliferative patterns—namely, trabecular, pseudoglandular, solid, and scirrhous patterns. We compared hypointense HCCs and iso- or hyperintense HCCs with regard to histologic features such as tumor differentiation, proliferation pattern, and the presence of bile plugs.

Polymerase Chain Reaction Analysis

The expression of OATP-A, OATP-B, OATP-C, OATP8, MRP1, MRP2 and MRP3 messenger RNA was examined by means of reverse transcription polymerase chain reaction (PCR) in HCCs and the surrounding liver tissue in 22 livers (Table 2) from which we could obtain fresh-frozen specimens. In the remaining 18 livers, the frozen specimens were not preserved. β-Actin was used as an internal reference. Primer sequences and product sizes are shown in Table E1 (online).

Next, we quantitatively examined messenger RNA expression levels of seven transporters in the same 22 livers by using real-time PCR. Specific primers and probes for seven transporters and β-actin were obtained from Applied Biosystems (Warrington, England). For quantitative evaluation of the expression of each transporter, we used the tumor/background expression score, defined as (tumor transporter value/tumor β-actin value)/(background transporter value/background β-actin value). Then, we examined the correlation of the transporter expression score and the enhancement ratio in the hepatobiliary phase of gadoxetic acid–enhanced MR imaging.

Immunohistochemical Analysis

According to the results of reverse transcription PCR, which indicated that OATP8 would be the key uptake transporter, immunostaining of OATP8 was performed for all HCCs by using a primary antibody against human OATP8 (mouse monoclonal, NB100–74482; Novus Biologicals, Littleton, Colo) (1:100). After removal of the specimen from the paraffin, antigen retrieval was performed by microwaving it in an edetic acid buffer (pH, 8.0) for 20 minutes. Two abdominal imaging radiologists (A.K. and N.Y. [with 7 years of experience]) semiquantitatively evaluated the intensity of OATP8 expression on the tumor cellular membrane in comparison with that of nonneoplastic hepatocytes as follows: A grade of 0 indicated no expression; a grade of 1+, decreased expression; a grade of 2+, equivalent expression; and a grade of 3+, increased expression. We used the grade at the largest area of each nodule.

Dual immunofluorescence staining of OATP8 and coagulation factor VIII, a marker of endothelial cells, was performed to examine whether or not OATP8 is expressed on the sinusoidal side of carcinoma cells. We used the previously described antibody for human OATP8 and rabbit polyclonal antibody for human factor VIII (A0082; Dako Cytomation, Glostrup, Denmark).

The details of the experiments (reverse transcription PCR and immunostaining) were as described in the article by Nakamura et al (28).

Overall Assessment

A schematic for the molecular background of the dynamics of gadoxetic acid in HCC cells as considered from our study was developed.

Statistical Analysis

Statistical significance was evaluated with software (Prism5; GraphPad Software, San Diego, Calif). The unpaired *t* test was used for the analysis of clinical features and quantitative reverse transcription PCR results, the Fisher exact test and the χ^2 test were used for the analysis of clinical and histologic features, the Friedman test was used for the time-SI curve, the Mann-Whitney test was used for the immunohistochemical findings, and the Pearson correlation test was used for the correlations between quantitative reverse transcription PCR and the enhancement ratio. $P < .05$ was considered to indicate a statistically significant difference.

Results

Clinical Features of the Two Types of HCCs

Thirty-two nodules were classified as hypointense HCCs, and eight nodules

Figure 2

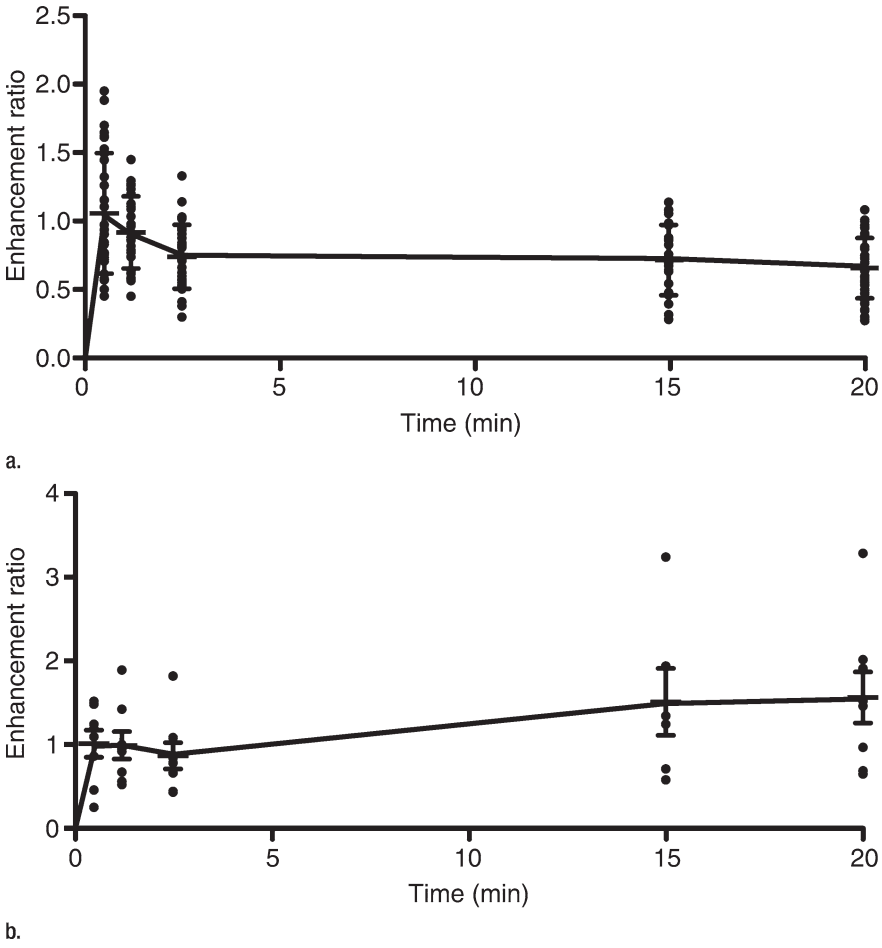

Figure 2: Time-SI curves at gadoxetic acid–enhanced MR imaging. Both hypointense HCCs and iso- or hyperintense HCCs show a rapid, increasing pattern in the arterial or the portal phase. **(a)** In hypointense HCCs, enhancement ratio decreases from the equilibrium phase to the hepatobiliary phase. **(b)** In contrast, iso- or hyperintense HCCs show increasing curves from the equilibrium phase to the hepatobiliary phase. $P < .001$. Enhancement ratio = (pre-enhancement SI minus postenhancement SI)/pre-enhancement SI.

were classified as iso- or hyperintense HCCs. No significant differences in any clinical features were observed between the two types (Table 1).

Time-SI Curves at Gadoxetic Acid–enhanced MR Imaging

Both the hypointense HCCs and the iso- or hyperintense HCCs showed a spike-like rapid increase of enhancement ratio in the arterial phase. After the equilibrium phase, the enhancement ratio decreased in hypointense HCCs; in contrast, iso- or hyperintense HCCs showed increasing intensity curves ($P < .001$) (Fig 2).

Messenger RNA Expression of Hepatocyte Membrane Transporters

OATP8 was constantly expressed in the background nonneoplastic portions of the livers. However, its expression was slight in all hypointense HCCs. In contrast, OATP8 expression was evident in all iso- or hyperintense HCCs (Fig 3). According to the results of real-time quantitative reverse transcription PCR (Fig 4; Fig E2 [online]), the degree of OATP8 expression in all hypointense HCCs was less than that in background livers (tumor/background expression score, <1.0), and was higher in iso- or hyperintense HCCs than in background livers (tumor/background expression score, >1.0) ($P < .001$).

The expression of MRP3, an export transporter on the sinusoidal side, was also lower in hypointense HCCs and was preserved in iso- or hyperintense HCCs, with a significant difference ($P < .001$). No significant difference was observed in the expression levels of the other transporters between the two types of HCCs ($P = .07–.53$). MRP2, a major export transporter on the canalicular side, was constantly expressed in all HCCs (Figs 3, 4; Fig E2 [online]).

There was a significant correlation between the tumor/background expression score of OATP8 and enhancement ratio in the hepatobiliary phase of gadoxetic acid–enhanced MR imaging ($P < .001$, $R = 0.84$) (Fig 5).

Immunohistochemistry of OATP8

In the nonneoplastic liver, OATP8 was expressed on the cellular membrane of hepatocytes at the sinusoidal side. In iso- or hyperintense HCCs, OATP8 was similarly expressed on the cellular membrane of HCC cells. In contrast, the degree of OATP8 expression in hypointense HCCs was clearly weaker than that in nonneoplastic liver ($P < .001$) (Figs 6, 7).

At double immunostaining of OATP8 and coagulation factor VIII in iso- or hyperintense HCCs, OATP8 was expressed on the sinusoidal side labeled by factor VIII in iso- or hyperintense HCCs (Fig E3 [online]). That is, in iso- or hyperintense HCCs, OATP8 expression was sustained on the cellular membrane at the sinusoidal side—the same as in nonneoplastic hepatocytes.

Pathologic Features of the Two Types of HCCs

Seven (88%) of eight iso- or hyperintense HCCs were moderately differentiated, and six (75%) of eight showed a predominantly pseudoglandular pattern, while seven (88%) of eight were associated with bile production (bile plugs). On the other hand, the hypointense HCCs consisted of three cases of well-differentiated, 25 cases of moderately differentiated, and four cases of poorly differentiated HCCs; the trabecular proliferation pattern was most

Table 2

Clinical, Histologic, and Radiologic Features in 22 Patients in Whom PCR Data Were Available

Patient Sex/Age (y)	Tumor Size (cm)	Differentiation	Proliferation Pattern	Bile Plugs	Gadoxetic Acid–enhanced MR Imaging Appearance
M/58	3.5	Moderate	Trabecular	Absent	Hypointense
M/77	14.5	Moderate	Pseudoglandular	Present	Hypointense
M/65	2.6	Moderate	Pseudoglandular	Present	Hypointense
M/78	8.8	Moderate	Solid	Absent	Hypointense
F/71	3.0	Moderate	Trabecular	Absent	Hypointense
M/60	2.5	Well	Pseudoglandular	Present	Hypointense
F/63	1.3	Well	Trabecular	Absent	Hypointense
F/60	1.8	Moderate	Trabecular	Absent	Hypointense
M/68	2.0	Well	Trabecular	Absent	Hypointense
M/63	3.8	Moderate	Trabecular	Absent	Hypointense
F/61	9.5	Moderate	Trabecular	Absent	Hypointense
M/60	5.2	Poor	Trabecular	Absent	Hypointense
M/52	7.2	Moderate	Trabecular	Absent	Hypointense
F/75	3.5	Moderate	Trabecular	Absent	Hypointense
F/63	3.3	Moderate	Pseudoglandular	Present	Hypointense
M/61	3.7	Moderate	Trabecular	Absent	Hypointense
M/57	2.0	Moderate	Trabecular	Absent	Hypointense
M/65	2.4	Moderate	Pseudoglandular	Present	Hyperintense
F/52	10.5	Moderate	Pseudoglandular	Present	Hyperintense
M/74	2.5	Well	Trabecular	Absent	Hyperintense
M/66	2.8	Moderate	Pseudoglandular	Present	Hyperintense
M/76	6.0	Moderate	Pseudoglandular	Present	Hyperintense

Figure 3

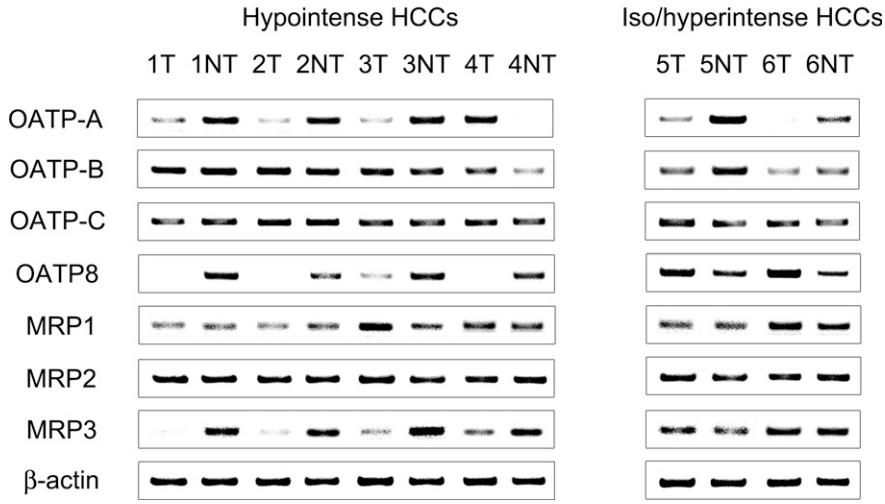

Figure 3: Results of reverse transcription PCR for hepatocellular transporters. Data in six typical cases of HCC are shown; the remaining cases also showed similar results. All transporters are almost constantly expressed in the background nonneoplastic livers. Expression of OATP8, an uptake transporter, is weak in hypointense HCCs (cases 1–4). In contrast, its expression in iso- or hyperintense HCCs is higher than that in background liver (cases 5–6). Expression of MRP3, an export transporter on the sinusoidal side, is also lower in hypointense HCCs and is preserved in iso- or hyperintense HCCs. There are no clear differences in the expression levels of the other five transporters (OATP-A, OATP-B, OATP-C, MRP1, and MRP2) between the two groups. *NT* = nontumor, *T* = tumor.

common (23 [72%] of 32 cases), whereas the pseudoglandular pattern and bile production were also observed in some cases (six [19%] and 10 [31%] cases, respectively). There was no significant difference compared with the occurrence in hypointense HCCs ($P = .57$). In contrast, there were significant differences in proliferation patterns and bile production between the two types of HCCs ($P = .01$ and $P = .006$, respectively) (Fig 8).

Figure 9 shows the molecular background of the dynamics of gadoxetic acid in HCC cells in our study. In iso- or hyperintense HCCs, a large amount of gadoxetic acid would be taken up from the tumor blood sinusoids into HCC cells by OATP8 and be gradually excreted again into tumor blood sinusoids by not MRP2 but MRP3, probably because of the depletion of bile ducts in the HCCs. On the other hand, the uptake of gadoxetic acid might be blocked or reduced because of the lower expression of OATP8 in hypointense HCCs.

Discussion

It has been reported that, uniquely among hepatic malignant tumors, some HCCs show iso- or hyperintensity in the hepatobiliary phase of gadoxetic acid–enhanced MR imaging (4,7). It has been suggested that this is reflective of the degree of residual hepatobiliary function or grade of tumor differentiation (11,12); however, to our knowledge, no basic studies are available to support these contentions. To clarify the mechanism underlying this finding, we performed an imaging-molecular-pathologic correlation study to compare HCCs that were hypointense to surrounding liver with those that were iso- or hyperintense.

Time-SI curves in hypointense HCCs showed a decrease in the SI of the tumor after the dynamic phase that continued to the hepatobiliary phase. This decreasing pattern corresponds to the so-called washout of contrast material from the tumor blood spaces commonly seen in hypervascular HCCs in the equilibrium phase of dynamic MR imaging with gadopentetate dimeglumine (10).

Figure 4

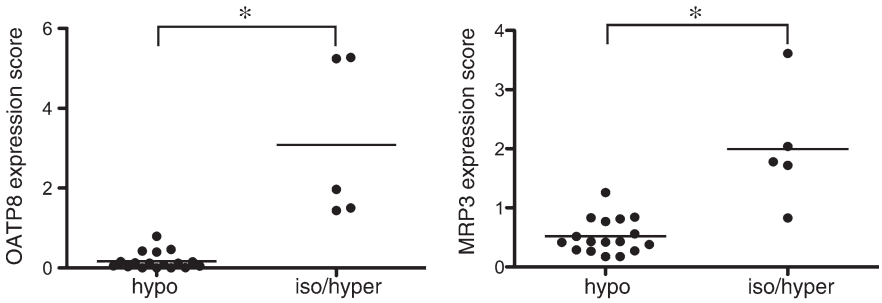

Figure 4: Graphs show results of quantitative real-time PCR of transporters. Hypointense HCCs *(hypo)* have significantly lower expression levels of **(a)** OATP8 and **(b)** MRP3 messenger RNA compared with iso- or hyperintense HCCs *(iso/hyper)* (* = $P < .001$). Expression score = (tumor transporter value/tumor β-actin value)/(background transporter value/background β-actin value). Tumor enhancement ratio = (pre-enhancement SI minus postenhancement SI)/pre-enhancement SI (in hepatobiliary phase).

Figure 5

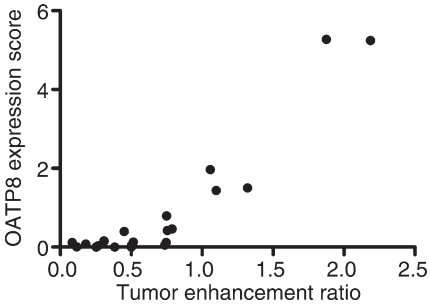

Figure 5: Correlation of OATP8 expression at PCR and tumor enhancement ratio in the hepatobiliary phase. There is a significant correlation between the tumor/background expression score of OATP8 and enhancement ratio in the hepatobiliary phase of gadoxetic acid–enhanced MR imaging. $P < .001$, $R = 0.84$. Expression score = (tumor transporter value/tumor β-actin value)/(background transporter value/background β-actin value). Enhancement ratio = (pre-enhancement SI minus postenhancement SI)/pre-enhancement SI.

This suggests that the decreasing pattern of the curve reflects the decline of the contrast medium in the tumor blood spaces and that the tumor cells hardly take up gadoxetic acid. In contrast, iso- or hyperintense HCCs demonstrated an increasing curve. This indicates that the uptake of gadoxetic acid is greater than the washout in iso- or hyperintense HCCs.

The PCR and immunostaining results showed that the OATP8 expression level was significantly higher in the iso- or hyperintense HCCs and significantly lower in hypointense HCCs than in the surrounding liver. In addition, the OATP8 expression level in HCCs was significantly and positively correlated with the enhancement ratio in the hepatobiliary phase of gadoxetic acid–enhanced MR imaging. Immunostaining also verified the location of OATP8 on the sinusoidal-side membrane of iso- or hyperintense HCC cells—the same as in nonneoplastic hepatocytes. On the basis of these results, we conclude that OATP8 is the best candidate among the four OATPs we tested to help determine the uptake of gadoxetic acid in HCC cells.

An important point is that particularly OATP8 is involved in the uptake of gadoxetic acid in HCC cells. Narita et al (29) recently reported similar results to ours. They also verified that there was a significant correlation between the enhancement ratio in the hepatobiliary phase and the expression level of OATP1B3 (synonymous with OATP8 [20]) protein at Western blot analysis in HCCs. However, their study focused solely on OATP1B3 and did not analyze the involvement of any other transporters. Therefore, the mechanisms of transporters in gadoxetic acid uptake were not elucidated in their entirety. We examined other possible transporters, because transporters can compensate to some extent for the functions of others, especially in disrupted conditions. Indeed, OATP8 and OATP-C share 80% of their amino acid sequences, and can transport some common substrates into cells (17). In our study, we showed that OATP8 and MRP3 expression correlated with enhancement ratio in HCCs, whereas the other five transporters containing OATP-C showed no significant correlations. However, it may be that the expression level does not always correspond with the functional level of a transporter. To examine the functional levels of OATP8 and the other transporters, further studies using cultures of purified hepatocytes from hypointense and iso- or hyperintense HCCs are needed.

MRP3 is an export transporter of organic anions on the sinusoidal side of hepatocytes. Its expression was significantly increased in iso- or hyperintense HCCs, which means that the excretion of gadoxetic acid from HCC cells into the tumor blood spaces (tumor sinusoids) is enhanced, probably because of the depletion of bile ducts in HCCs. We surmise this to be a reactive response to the increase in OATP8 expression, to export more substrate into blood. In contrast, the excretion by MRP2, the transporter on the canalicular side, would not function in HCCs, because there are few larger bile ducts in tumor tissue. Therefore, the efflux of gadoxetic acid into tumor blood spaces would appear to be the main route of excretion from HCC cells in iso- or hyperintense HCCs. The rate of excretion is likely to be slower than the rate of uptake and thus to hardly influence the SI in the hepatobiliary phase of gadoxetic acid–enhanced MR imaging.

We also analyzed the histologic differences between hypointense HCCs and iso- or hyperintense HCCs. The majority of iso- or hyperintense HCCs were moderately differentiated HCCs; this may be due to genetic reversion to their original hepatocyte nature during hepatocarcinogenesis because, as shown by Tsuda et al (30), the ability of tumor cells to take up gadoxetic acid would be expected to be lost during the early stage of hepatocarcinogenesis in rats. Interestingly, iso- or hyperintense HCCs showed pseudoglandular proliferation

Figure 6

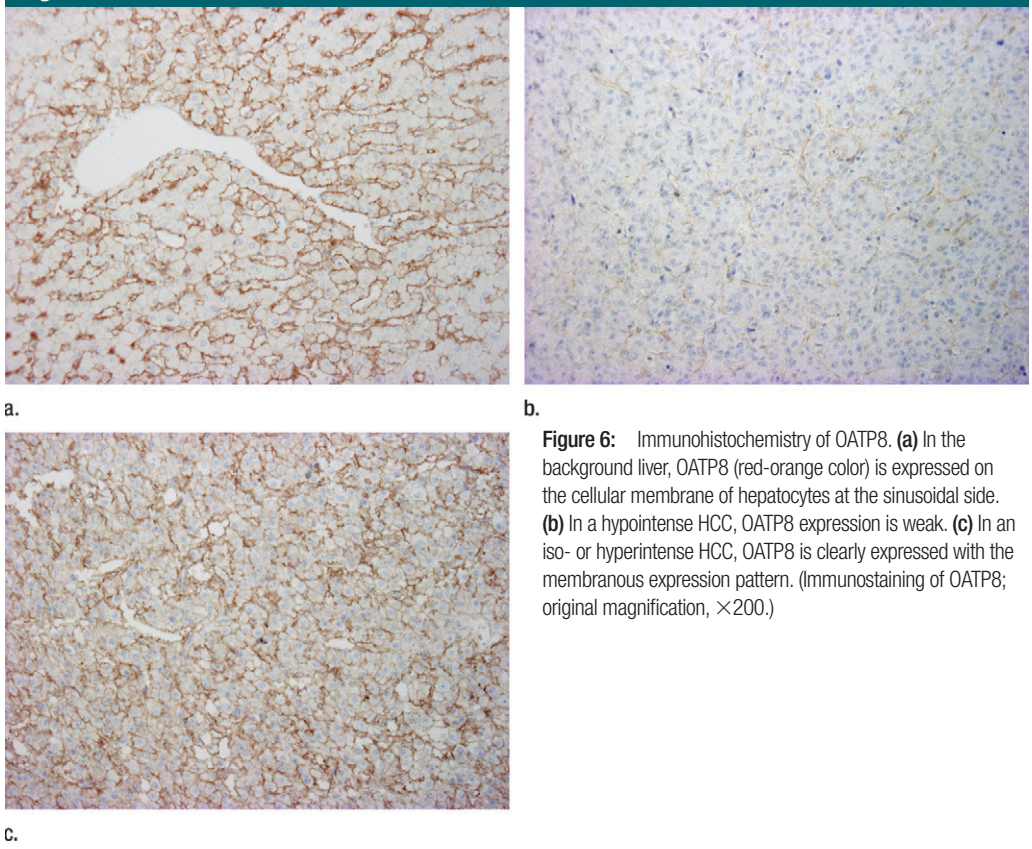

Figure 6: Immunohistochemistry of OATP8. **(a)** In the background liver, OATP8 (red-orange color) is expressed on the cellular membrane of hepatocytes at the sinusoidal side. **(b)** In a hypointense HCC, OATP8 expression is weak. **(c)** In an iso- or hyperintense HCC, OATP8 is clearly expressed with the membranous expression pattern. (Immunostaining of OATP8; original magnification, ×200.)

Figure 7

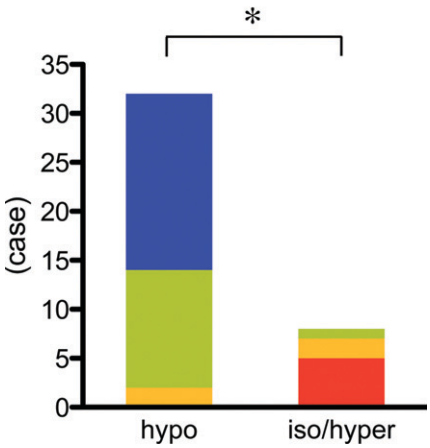

Figure 7: Bar graph shows results of semiquantitative analysis of the immunohistochemistry of OATP8. OATP8 expression in iso- or hyperintense HCCs *(iso/hyper)* is significantly extensive compared with that in hypointense HCCs *(hypo)* (* = $P < .001$, Mann-Whitney test). Blue = no expression, green = decreased expression, yellow = equivalent expression, red = increased expression.

with bile plugs with significantly high frequency, suggesting overproduction of bile and secondary dilatation of bile canaliculi (31). Overexpression of OATP8 might contribute to the overproduction of bile, because OATP8 can take up bile acid components. However, this proliferation pattern was also fairly often seen in hypointense HCCs. It is difficult to directly correlate the expression levels of OATP8 and the quantity of bile production, because nonanion transporters such as Na^+/taurocholate cotransporting polypeptide and organic cation transporter also participate in bile production (32).

Benign hepatocellular nodules, like focal nodular hyperplasia, commonly show isointensity or hyperintensity in the hepatobiliary phase (4–6). We suppose that uptake transporters, including OATP8 and export transporters, are expressed normally or increasingly in these hyperplastic cells. However, the SI may be determined by the expression of uptake transporters rather than that of export transporters, as shown in our study. Radiologic-pathologic studies of benign or premalignant hepatocellular nodules performed with similar methods are needed to clarify this issue.

Our study had several limitations. First, the total number of iso- or hyperintense HCCs examined was small because such tumors are relatively rare, and reverse transcription PCR was performed in only 22 of 40 HCCs from which we could obtain fresh-frozen specimens. Second, we simply divided HCCs into hypointense and iso- or hyperintense type according to the average SI in the maximum ROI for this analysis. In the future, it will be important to correlate each area of different SI with tumor differentiation, proliferation pattern, or the expression of transporters in heterogeneous lesions. However, we believe that the data obtained are sufficient to make conclusions about the molecular biology of gadoxetic acid–enhanced MR imaging pharmacodynamics, because the expression levels

Figure 8

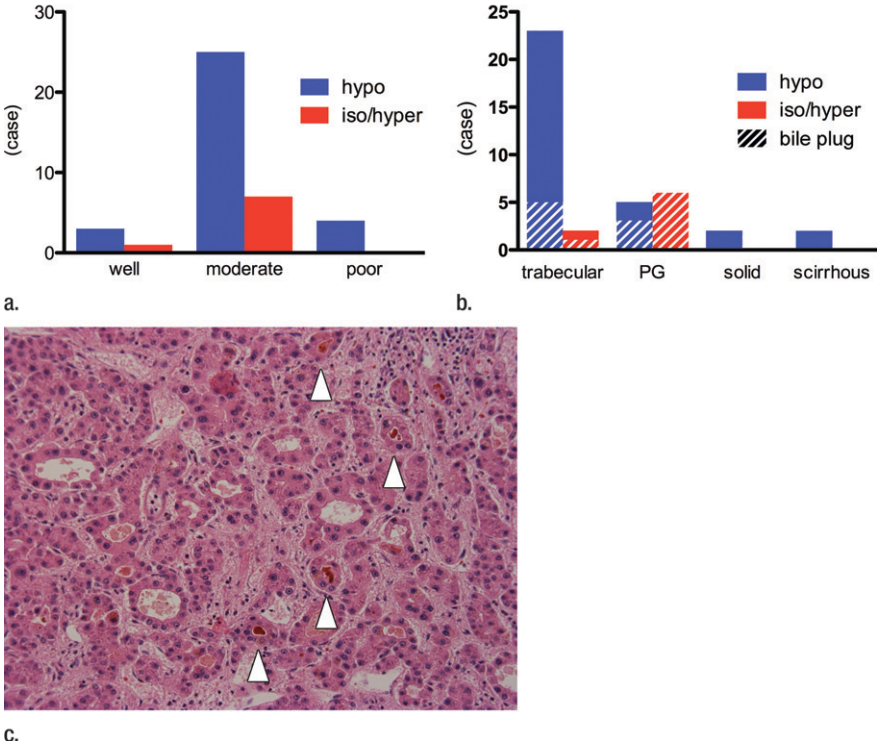

Figure 8: Histologic proliferation patterns of HCCs. **(a)** Graph shows tumor differentiation. The hypointense HCCs *(hypo)* consisted of well-differentiated (9%), moderately differentiated (78%), and poorly differentiated HCCs (12%), while 88% of iso- or hyperintense HCCs *(iso/hyper)* were moderately differentiated. **(b)** Graph shows tumor proliferation pattern. Seventy-five percent of iso- or hyperintense HCCs had a pseudoglandular pattern, and 88% showed bile plugs. In the hypointense HCCs, the trabecular pattern was most common; in addition, a pseudoglandular *(PG)* proliferation pattern and bile production were observed in 19% and 31% of nodules, respectively. There was no significant difference in tumor differentiation ($P = .57$), while there were significant differences in proliferation patterns or bile production between the two types of HCCs ($P = .01$ and $P = .006$, respectively). **(c)** A case of iso- or hyperintense HCC shows a pseudoglandular pattern with bile production (arrowheads). (Hematoxylin-eosin stain; original magnification, ×200.)

Figure 9

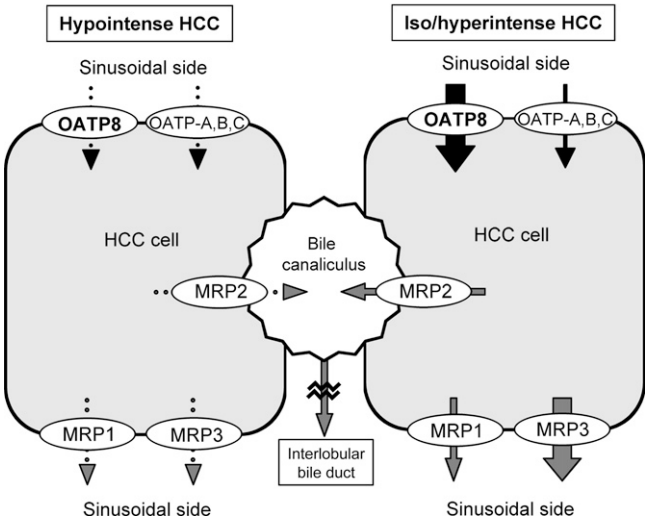

Figure 9: Schematic of transporter expression and mechanism of gadoxetic acid dynamics in HCC. Between hypointense and iso- or hyperintense HCCs, the most significant differences were observed in OATP8 and MRP3 expression. That is, in iso- or hyperintense HCCs, a larger amount of gadoxetic acid would be taken up from the tumor blood sinusoids into HCC cells by OATP8 and be excreted again into tumor blood sinusoids by MRP3 very gradually, probably because of the depletion of bile ducts in the HCCs. In contrast, in hypointense HCCs, the uptake of gadoxetic acid might be blocked or reduced because of the lower expression of OATP8.

of OATP8 and MRP3 and the time-SI curves showed significant differences between the two types of HCCs. Third, patients with poor liver function were not included in this study. The relative SI in the hepatobiliary phase would be modified in these patients; for example, HCC without OATP8 expression could be visualized as isointense. Therefore, the liver function of patients should be considered when evaluating the SI of HCCs (33,34).

In conclusion, the expression of the uptake transporter OATP8 and the export transporter MRP3 in HCC cells significantly correlated with the SI of HCCs in the hepatobiliary phase of gadoxetic acid–enhanced MR imaging. In human HCC cells, OATP8 and MRP3 are probably the uptake transporter and export transporter of gadoxetic acid, respectively.

References

1. Vogl TJ, Kümmel S, Hammerstingl R, et al. Liver tumors: comparison of MR imaging with Gd-EOB-DTPA and Gd-DTPA. Radiology 1996;200(1):59–67.

2. Huppertz A, Balzer T, Blakeborough A, et al. Improved detection of focal liver lesions at MR imaging: multicenter comparison

of gadoxetic acid-enhanced MR images with intraoperative findings. Radiology 2004; 230(1):266–275.

3. Bluemke DA, Sahani D, Amendola M, et al. Efficacy and safety of MR imaging with liver-specific contrast agent: U.S. multicenter phase III study. Radiology 2005;237(1):89–98.
4. Huppertz A, Haraida S, Kraus A, et al. Enhancement of focal liver lesions at gadoxetic acid-enhanced MR imaging: correlation with histopathologic findings and spiral CT—initial observations. Radiology 2005; 234(2):468–478.
5. Zech CJ, Herrmann KA, Reiser MF, Schoenberg SO. MR imaging in patients with suspected liver metastases: value of liver-specific contrast agent Gd-EOB-DTPA. Magn Reson Med Sci 2007;6(1):43–52.
6. Reimer P, Schneider G, Schima W. Hepatobiliary contrast agents for contrast-enhanced MRI of the liver: properties, clinical development and applications. Eur Radiol 2004; 14(4):559–578.
7. Saito K, Kotake F, Ito N, et al. Gd-EOB-DTPA enhanced MRI for hepatocellular carcinoma: quantitative evaluation of tumor enhancement in hepatobiliary phase. Magn Reson Med Sci 2005;4(1):1–9.
8. Schuhmann-Giampieri G, Schmitt-Willich H, Press WR, Negishi C, Weinmann HJ, Speck U. Preclinical evaluation of Gd-EOB-DTPA as a contrast agent in MR imaging of the hepatobiliary system. Radiology 1992;183(1):59–64.
9. Hamm B, Staks T, Mühler A, et al. Phase I clinical evaluation of Gd-EOB-DTPA as a hepatobiliary MR contrast agent: safety, pharmacokinetics, and MR imaging. Radiology 1995;195(3):785–792.
10. Hecht EM, Holland AE, Israel GM, et al. Hepatocellular carcinoma in the cirrhotic liver: gadolinium-enhanced 3D T1-weighted MR imaging as a stand-alone sequence for diagnosis. Radiology 2006;239(2):438–447.
11. Reimer P, Rummeny EJ, Daldrup HE, et al. Enhancement characteristics of liver metastases, hepatocellular carcinomas, and hemangiomas with Gd-EOB-DTPA: preliminary results with dynamic MR imaging. Eur Radiol 1997;7(2):275–280.
12. Bartolozzi C, Crocetti L, Lencioni R, Cioni D, Della Pina C, Campani D. Biliary and reticuloendothelial impairment in hepatocarcinogenesis: the diagnostic role of tissue-specific MR contrast media. Eur Radiol 2007; 17(10):2519–2530.
13. van Montfoort JE, Stieger B, Meijer DK, Weinmann HJ, Meier PJ, Fattinger KE. Hepatic uptake of the magnetic resonance imaging contrast agent gadoxetate by the organic anion transporting polypeptide Oatp1. J Pharmacol Exp Ther 1999;290(1): 153–157.
14. Lorusso V, Pascolo L, Fernetti C, Visigalli M, Anelli P, Tiribelli C. In vitro and in vivo hepatic transport of the magnetic resonance imaging contrast agent B22956/1: role of MRP proteins. Biochem Biophys Res Commun 2002;293(1):100–105.
15. Abe T, Kakyo M, Tokui T, et al. Identification of a novel gene family encoding human liver-specific organic anion transporter LST-1. J Biol Chem 1999;274(24): 17159–17163.
16. Hsiang B, Zhu Y, Wang Z, et al. A novel human hepatic organic anion transporting polypeptide (OATP2). Identification of a liver-specific human organic anion transporting polypeptide and identification of rat and human hydroxymethylglutaryl-CoA reductase inhibitor transporters. J Biol Chem 1999;274(52):37161–37168.
17. König J, Cui Y, Nies AT, Keppler D. Localization and genomic organization of a new hepatocellular organic anion transporting polypeptide. J Biol Chem 2000;275(30): 23161–23168.
18. Kullak-Ublick GA, Ismair MG, Stieger B, et al. Organic anion-transporting polypeptide B (OATP-B) and its functional comparison with three other OATPs of human liver. Gastroenterology 2001;120(2):525–533.
19. Kullak-Ublick GA, Hagenbuch B, Stieger B, et al. Molecular and functional characterization of an organic anion transporting polypeptide cloned from human liver. Gastroenterology 1995;109(4):1274–1282.
20. Vavricka SR, Jung D, Fried M, Grützner U, Meier PJ, Kullak-Ublick GA. The human organic anion transporting polypeptide 8 (SLCO1B3) gene is transcriptionally repressed by hepatocyte nuclear factor 3beta in hepatocellular carcinoma. J Hepatol 2004;40(2): 212–218.
21. Zhou SF, Wang LL, Di YM, et al. Substrates and inhibitors of human multidrug resistance associated proteins and the implications in drug development. Curr Med Chem 2008; 15(20):1981–2039.
22. Müller M, Roelofsen H, Jansen PL. Secretion of organic anions by hepatocytes: involvement of homologues of the multidrug resistance protein. Semin Liver Dis 1996;16(2): 211–220.
23. Tsujii H, König J, Rost D, Stöckel B, Leuschner U, Keppler D. Exon-intron organization of the human multidrug-resistance protein 2 (MRP2) gene mutated in Dubin-Johnson syndrome. Gastroenterology 1999; 117(3):653–660.
24. König J, Rost D, Cui Y, Keppler D. Characterization of the human multidrug resistance protein isoform MRP3 localized to the basolateral hepatocyte membrane. Hepatology 1999;29(4):1156–1163.
25. Zech CJ, Vos B, Nordell A, et al. Vascular enhancement in early dynamic liver MR imaging in an animal model: comparison of two injection regimen and two different doses Gd-EOB-DTPA (gadoxetic acid) with standard Gd-DTPA. Invest Radiol 2009;44(6): 305–310.
26. Terminology of nodular hepatocellular lesions. International Working Party. Hepatology 1995;22(3):983–993.
27. Hirohashi S, Ishak KG, Kojiro M, et al. Hepatocellular carcinoma. In: Hamilton SR, Aaltonen LA, eds. Pathology and genetics of tumours of the digestive system. Lyon, France: IARC, 2000; 157–172.
28. Nakamura K, Zen Y, Sato Y, et al. Vascular endothelial growth factor, its receptor Flk-1, and hypoxia inducible factor-1alpha are involved in malignant transformation in dysplastic nodules of the liver. Hum Pathol 2007;38(10):1532–1546.
29. Narita M, Hatano E, Arizono S, et al. Expression of OATP1B3 determines uptake of Gd-EOB-DTPA in hepatocellular carcinoma. J Gastroenterol 2009;44(7):793–798.
30. Tsuda N, Kato N, Murayama C, Narazaki M, Yokawa T. Potential for differential diagnosis with gadolinium-ethoxybenzyl-diethylenetriamine pentaacetic acid-enhanced magnetic resonance imaging in experimental hepatic tumors. Invest Radiol 2004;39(2):80–88.
31. Kondo Y, Nakajima T. Pseudoglandular hepatocellular carcinoma. A morphogenetic study. Cancer 1987;60(5):1032–1037.
32. Kullak-Ublick GA, Beuers U, Paumgartner G. Hepatobiliary transport. J Hepatol 2000; 32(1 suppl):3–18.
33. Ryeom HK, Kim SH, Kim JY, et al. Quantitative evaluation of liver function with MRI Using Gd-EOB-DTPA. Korean J Radiol 2004;5(4):231–239.
34. Kim T, Murakami T, Hasuike Y, et al. Experimental hepatic dysfunction: evaluation by MRI with Gd-EOB-DTPA. J Magn Reson Imaging 1997;7(4):683–688.